ASM Sc. J., 11, Special Issue 2, 2018 for SANREM, 189-195

# Modification in Structural and Optical Properties of Erbium-doped Zinc Sodium Tellurite Glass: Effect of Bimetallic Nanoparticles

Asmahani Awang[1*], Khasidah Kamarudin[1], S. Nurhajra Piara[1], C.F. Pien[1] and Jedol Dayou[2]

[1]*Physics with Electronics Programme, Faculty of Science and Natural Resources, Universiti Malaysia Sabah, 88400 Kota Kinabalu, Sabah, Malaysia.*

[2]*Energy, Vibration and Sound Research Group (e-VIBS), Faculty of Science and Natural Resources, Universiti Malaysia Sabah, 88400 Kota Kinabalu, Sabah, Malaysia*

The demand in accomplishing modified structural and optical features of trivalent rare earth (RE) ions doped amorphous media through the incorporation of metallic nanoparticles (NPs) of controlled sizes is ever-increasing for short wavelength solid state lasers development. In this view, we attempt to alter the optical properties of bimetallic NPs and erbium ($Er^{3+}$) integrated zinc-sodium-tellurite glass. Modifications in structural properties are triggered via precise control of titanium and copper NPs nucleation and growth processes underneath the amorphous matrix. The changes in ligand interactions in the fragile disordered matrix are found to be accountable for the variations in structural and optical properties. A series of glass with composition of $(70\text{-}x\text{-}y)TeO_2\text{-}20ZnO\text{-}9Na_2O\text{-}1Er_2O_3\text{-}(x)CuO\text{-}(y)TiO_2$ (x = 0.0 and 0.04 mol%; y = 0.0 and 0.1 mol%) are prepared following melt-quenching method and characterized. UV-Vis-NIR spectra displayed seven absorption bands corresponding to the transitions from ground state ($^4I_{15/2}$) to $^4F_{5/2}$, $^4F_{7/2}$, $^2H_{11/2}$, $^4S_{3/2}$, $^4F_{9/2}$, $^4I_{9/2}$ and $^4I_{11/2}$ excited states of $Er^{3+}$. FTIR spectra show the presence of symmetric Te-O-Te linkage vibrations and stretching vibrations of Cu-O on monoclinic CuO, Te-O bond of the trigonal bypiramidal unit [$TeO_4$] with non-bridging oxygen symmetrical $TeO_3$ groups and vibrations of water molecule. The presence of bimetallic NPs is confirmed from transmission electron microscopy (TEM) imaging. Our glass composition demonstrating such significant modification in structural and optical properties may be beneficial for the development of plasmonic devices.

**Keywords:** Bimetallic, nanoparticles, amorphous, glass, growth

## I. INTRODUCTION

Tellurite glass exhibits large infrared transparency, high linear and non-linear refractive indices, good thermal stability, corrosion resistance and suitability as a matrix for active element doping. The beneficial features represent the main justification for their continuous technological interest (Jlassi *et al.,* 2011). The spectroscopic investigation of tellurite glass containing metallic NPs attracts large interest due to controlled optical properties of materials by appropriate thermal treatment (Kassab *et al.*, 2008). The sharp edges

*Corresponding author's e-mail: asmahani_awang@yahoo.com

of NPs act as light-harvesting nano-optical antennas converting visible light into a large localized electric field mainly known as lightning-rod effect (Som & Karmakar, 2009).

However, the controlled production of bimetallic NPs embedded in glasses matrix is a current challenge with promissory applications (Singh *et al.,* 2010). Conventional methods of incorporating metallic NPs within glasses involve multistep techniques like ion implantation, ion exchange, and subsequent heat treatment in reducing atmosphere (Singh *et al.,* 2010). Significantly, the addition of titanium and copper from two different metal ions facilitates the generation of an optical responses (Tao *et al*., 2015). Generally, titanium can improve the stability of glass structure and copper exhibits good thermal and electrical conductivity (Wers *et al.,* 2014). In present study, we report the influence of controlled concentrations of bimetallic NPs and nanocluster dimensions inside the glass host responsible for tailoring the optical and structural properties of glass.

## II. MATERIALS AND METHODS

Series of glasses (enlisted in Table 1) with nominal composition (70-x-y)$TeO_2$-20ZnO-9$Na_2O$-1$Er_2O_3$-(x)CuO-(y)$TiO_2$ (x = 0.0 and 0.04 mol%; y = 0.0 and 0.1 mol%) are synthesized using melt-quenching technique. Starting materials of $TeO_2$, ZnO, $Na_2O$, $Er_2O_3$, $TiO_2$ and CuO from Sigma Aldrich with 99.9% purity are mixed thoroughly. A platinum crucible containing the glass constituents is placed in a furnace from room temperature up to 900 °C for 25 min and the melt is placed in a brass mould after melting process.

Subsequently, the sample was transferred to an annealing furnace and kept for 3 hours at 295 °C to remove the thermal and mechanical strains completely. The samples are then cooled down to room temperature. Finally, the samples were cut and polished for the structural and optical measurements. The room temperature absorption spectra in the range of 400 – 1100 nm are recorded by using Agilent Technologies Cary 60 UV-Vis. The FTIR spectra are recorded by using FTIR Spectrum 100. The transmission electron microscope of TECNAI G2 Spirit Biotwint working at 120 kV is employed to image the existence and growth of bimetallic NPs of distinct sizes.

Table 1. The glass composition (mol%) of studied glasses

| Glass | $TeO_2$ | ZnO | $Na_2O$ | $Er_2O_3$ | $TiO_2$ | CuO |
|---|---|---|---|---|---|---|
| TZNE | 70 | 20 | 9 | 1 | - | - |
| TZNECu | 69.9 | 20 | 9 | 1 | - | 0.1 |
| TZNETi | 69.9 | 20 | 9 | 1 | 0.1 | - |
| TZNECuTi | 69.86 | 20 | 9 | 1 | 0.1 | 0.04 |

## III. RESULTS AND DISCUSSIONS

Lorem ipsum dolor sit amet, consectetur The room temperature UV-Vis-NIR absorption spectra of $Er_2O_3$ doped tellurite glasses in Figure 1. The spectra comprised of seven absorption bands centered at 447, 490, 519, 546, 653, 798 and 977 nm corresponding to the transitions from the ground state $^4I_{15/2}$ of $Er^{3+}$ ions to $^4F_{5/2}$, $^4F_{7/2}$, $^2H_{11/2}$, $^4S_{3/2}$,$^4F_{9/2}$, $^4I_{9/2}$ and $^4I_{11/2}$ excited states, respectively. Table 2 summarizes all the observed absorption bands.

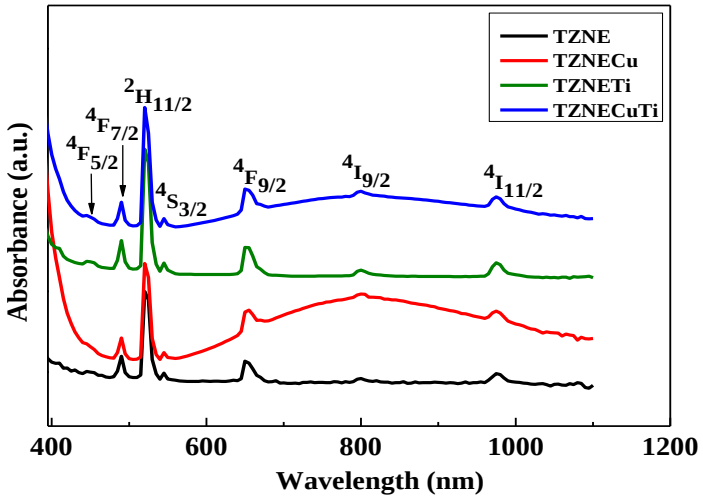


Figure 1. UV-Vis absorption spectra of glass samples in range of 400 – 1100 nm

Table 2. Peak positions in ultraviolet-visible range of different glass samples.

| Peak position (nm) | Energy ($cm^{-1}$) | Erbium transition |
|---|---|---|
| 447 | 22371 | $^4I_{15/2} \rightarrow {}^4F_{5/2}$ |
| 490 | 20408 | $^4I_{15/2} \rightarrow {}^4F_{7/2}$ |
| 519 | 19268 | $^4I_{15/2} \rightarrow {}^2H_{11/2}$ |
| 546 | 18315 | $^4I_{15/2} \rightarrow {}^4S_{3/2}$ |
| 653 | 15314 | $^4I_{15/2} \rightarrow {}^4F_{9/2}$ |
| 798 | 12531 | $^4I_{15/2} \rightarrow {}^4I_{9/2}$ |
| 977 | 10235 | $^4I_{15/2} \rightarrow {}^4I_{11/2}$ |

The FTIR spectra displayed in Figure 2 provides information concerning various bonding among different ions in the glass network. Table 3 summarizes the observed peaks in the entire spectral region and their corresponding band assignments. The occurrence of broad band is attributed to the contribution of higher degenerate vibrational states, thermal broadening of the lattice dispersion and mechanical scattering from the powdered samples (Singh *et al.,* 2010). Fundamentally, the structure of $TeO_2$ rich glasses contains three dimensional networks of $TeO_4$ tbp units with oxygen at two equatorial and axial sites in which the other equatorial site being occupied by a lone pair of electrons. The incorporation of RE ions creates asymmetric $TeO_4$ polyhedron with one short, three elongated Te–O bonds and $TeO_3$ trigonal pyramids having NBO. The bond dipole results from the bond length and the charge difference between the two atoms (de Araújo *et al.,* 2013).

The appearance of bands in 443 – 496 $cm^{-1}$ region are allocated to ZnO bond vibration. Generally, the absorption band centered at 640 $cm^{-1}$ is the characteristic of pure $TeO_2$ glass (Pavani *et al.,* 2011). However, in this study the existence of two bands around 578 – 592 $cm^{-1}$

and 677 $cm^{-1}$ are assigned to the $TeO_4$ and $TeO_3$ structural units, respectively (Xu *et al.,* 2011). The broadening of these bands with respect to the crystalline $TeO_2$ is apparent due to wide distribution of bond angles and lengths in the amorphous matrix (Dousti *et al.,* 2013). The bands at around 1180 – 1226 $cm^{-1}$ are attributed to vibrations of water molecule. The appearance of copper and titanium bonding are not observed in FTIR spectra due to a lower concentration of copper and titanium. However, the distribution of copper and titanium NPs in glass matrix are confirmed by using TEM as discussed further in the next section.

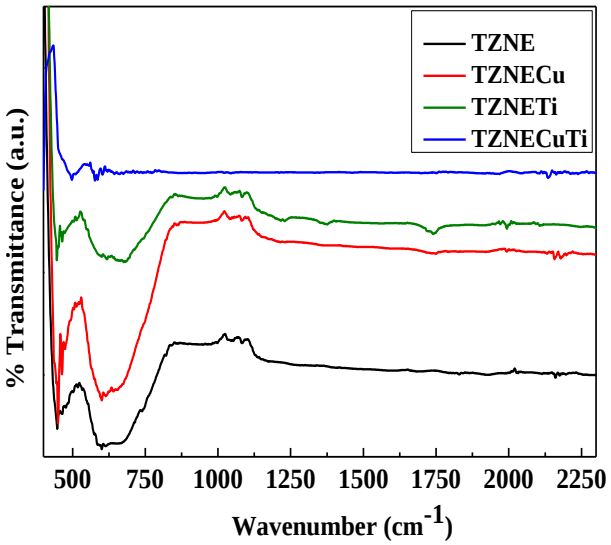


Figure 2. FTIR spectra of glass in therange of 400 – 2300 $cm^{-1}$

Table 3. IR band assignments of different glass samples with varying concentration of dopants.

| Glass code | | | | Band assignments |
|---|---|---|---|---|
| TZNE ($cm^{-1}$) | TZNECu ($cm^{-1}$) | TZNETi ($cm^{-1}$) | TZNECuTi ($cm^{-1}$) | |
| 443 | 443 | 443 | 496 | Vibrations of Zn-O tetrahedral bond ($ZnO_4$) and stretching vibrations of Cu-O on monoclinic CuO |
| 592 | 592 | 592 | 578 | Te-O bending stretching vibrations in $TeO_4$ units |
| 677 | 677 | 677 | - | Te-O bending vibrations in $TeO_3$ units |
| 1180 | 1209 | 1226 | - | Vibrations of water molecule |

TEM micrograph as shown in Figure 3 reveals the presence of non-spherical NPs in the glass matrix. The black spots verify the occurrence of metallic NPs having different sizes and shapes. Figure 3(a), 3(b) and 3(c) represents the formation of Cu NPs, Ti NPs and CuTi NPs with varying sizes and aspect ratio. The range of aspect ratio for Cu NPs is discerned to be from 1.07 to 3.20. Meanwhile, the range of aspect ratio for Ti NPs is found in range of 1.19 to 1.28. Finally, the formation of bimetallic CuTi NPs shows the inner and outer diameter of 36.05 and 4.25 nm, respectively. Table 4 and 5 summarize the detailed information for varying sizes in terms of transverse diameter and longitudinal diameter for monometallic Cu and Ti NPs, in addition of inner and outer diameter of bimetallic CuTi NPs.

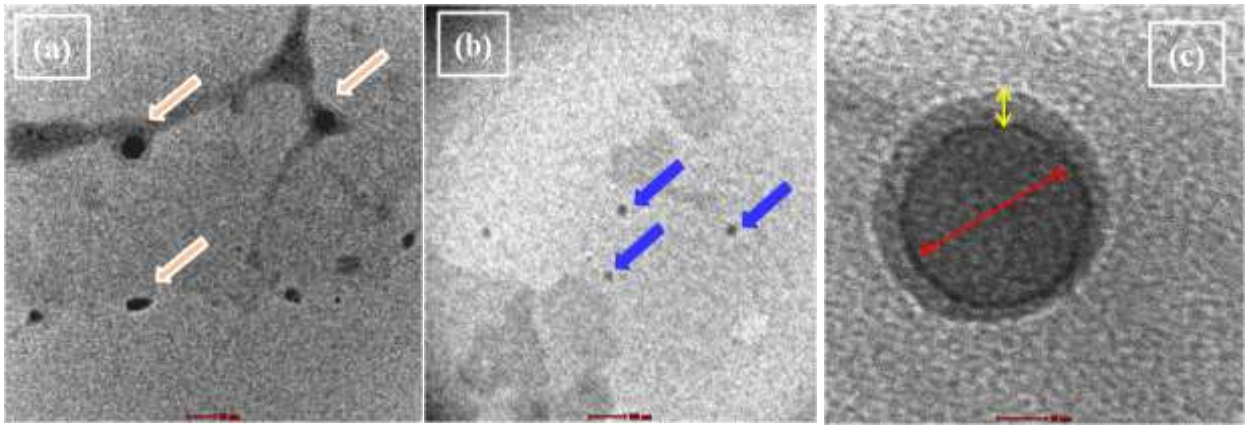


Figure 3. TEM images of the glass sample of shows the formation of (a) Cu NPs (b) Ti NPs and (c) bimetallic CuTi NPs

Table 4. Size distribution in of respective Cu and Ti NPs in glass matrix

| Glass code | Diameter (nm) | | Aspect ratio |
|---|---|---|---|
| | Transverse | Longitudinal | |
| TZNECu | 18.14 | 19.61 | 1.08 |
| | 12.25 | 21.57 | 1.76 |
| | 20.10 | 21.57 | 1.07 |
| | 32.84 | 39.71 | 1.21 |
| | 9.87 | 31.58 | 3.20 |
| TZNETi | 19.08 | 24.34 | 1.28 |
| | 20.39 | 24.34 | 1.19 |
| | 18.18 | 25.76 | 1.42 |
| | 23.03 | 27.63 | 1.20 |

Table 5. Inner and outer size of bimetallic NPs

| TZNECuTi | Diameter (nm) | |
|---|---|---|
| | Inner | Outer |
| | 36.05 | 4.25 |

## IV. SUMMARY

We demonstrate the modification in the structural properties of tellurite glass via incorporation of bimetallic NPs in a small concentration. In current study, we manage to achieve the formation of core-shell bimetallic NPs of CuTI which is beneficial to modify the structural and optical properties of glass. The formations of CuTi bimetallic NPs distribute in the glass matrix are found to be 36.05 nm for inner diameter and 4.25 nm for outer diameter. The FTIR spectra revealed the network structure consisting of vibrational $ZnO_4$ bonds, Te-O bond in $TeO_3$ tbp, $TeO_4$ tbp unit and the vibrations of water molecule without

displaying the existence of Ti in glass matrix. inner diameter and 4.25 nm for outer diameter. The FTIR spectra revealed the network structure consisting of vibrational $ZnO_4$ bonds, Te-O bond in $TeO_3$ tbp, $TeO_4$ tbp unit and the vibrations of water molecule without displaying the existence of Ti in glass matrix.

## V. ACKNOWLEDGMENT

The authors wish to thank to UMS, UTM and Ministry of Higher Education (MoHE) for the financial support through SGPUMS grant (SGK0008-SG-2015), Project Research Acculturation Grant Scheme (RAG-0067-SG-2015) and GUG0130-1/2017

[1] de Araújo, CB, Oliveira, TR, Falcão-Filho, EL, Silva, DM & Kassab, LR 2013, 'Nonlinear optical properties of PbO–GeO2 films containing gold nanoparticles', Journal of Luminescence, vol. 133, pp. 180-183.

[2] Dousti, MR, Sahar, MR, Ghoshal, SK, Amjad, RJ & Samavati, AR 2013, 'Effect of AgCl on spectroscopic properties of erbium doped zinc tellurite glass', Journal of Molecular Structure, vol. 1035, pp. 6-12.

[3] Jlassi, I, Elhouichet, H & Ferid, M 2011, 'Thermal and optical properties of tellurite glasses doped erbium', Journal Materials Science, vol. 46, no. 3, pp. 806-812.

[4] Kassab, LR, de Almeida, R, da Silva, DM & de Araújo, CB 2008, 'Luminescence of Tb 3+ doped TeO 2–ZnO–Na 2 O– PbO glasses containing silver nanoparticles', Journal of Applied Physics, vol. 104, no. 9, 093531.

[5] Pavani, PG, Sadhana, K & Mouli, VC 2011, 'Optical, physical and structural studies of boro-zinc tellurite glasses', Physica B: Condensed Matter, vol. 4 06(6-7), pp. 1242-1247.

[6] Singh, SK, Giri, NK, Rai, DK & Rai, SB 2010, 'Enhanced upconversion emission in Er3+-doped tellurite glass containing silver nanoparticles' Solid State Sciences, vol. 12, no. 8, pp. 1480- 1483.

[7] Som, T & Karmakar, B 2009, ' Enhancement of Er 3+ upconverted luminescence in Er 3+: Au-antimony glass dichroic nanocomposites containing hexagonal Au nanoparticles', Journal of the Optical Society of America B, vol. 26, no. 12, pp. 21-27.

[8] Tao, C, Jia, G, Mu, X, Dai, H & Liu, C 2015, 'Synthesis and Optical Properties of Cu Core/Ti-Related Shell Nanoparticles in Silica Sequentially Implanted With Ti and Cu Ions', Plasmonics, vol.10, no. 6, pp. 1869-1876.

[9] Wers, E, Oudadesse, H, Lefeuvre, B, Lucas-Girot, A, Rocherullé, J & Lebullenger, R 2014, 'Excess entropy and thermal behavior of Cu-and Ti-doped bioactive glasses', Journal of Thermal Analysis and Calorimetry, vol. 117, no. 2, pp. 579-588.

[10] Xu, T, Chen, F, Dai, S, Shen, X, Wang, X, Nie, Q & Heo, J 2011, 'Glass formation and third-order optical nonlinear properties within TeO2–Bi2O3–BaO pseudo-ternary system, Journal of Non-Crystalline Solids, vol. 357, no. 11-13, pp. 2219-2222.